Parameter identification and trajectory following of a two-link rigid manipulator

R Fotouhi-C, W Szyszkowski, P N Nikiforuk* and **M M Gupta**
Mechanical Engineering Department, University of Saskatchewan, Saskatoon, Saskatchewan, Canada

Abstract: An adaptive controller for rigid manipulators is discussed in this paper. The scheme presented is applied to a two-link rigid manipulator. It takes full advantage of the known parameters of the manipulator while estimating the unknown parameters. In deriving the dynamic equations of motion, all the physical parameters of the manipulator, including the distributed masses of the links, are taken into account. The overall control system maintains the structure of the computed torque system with an adaptive element. The convergence of the control is considered in detail. A method of selecting the best combination of the various gains is presented. Some simulation results of the manipulator with unknown payload masses following a desired trajectory are presented.

Keywords: adaptive control, rigid manipulator, path following

NOTATION

a_{11}	non-linear function of rotation
a_{12}	non-linear function of rotation
a_{13}	non-linear function of rotation
a_{14}	non-linear function of rotation
a_{22}	constant
a_{24}	non-linear function of rotation
$\mathbf{A}$	constant matrix
$\mathbf{B}$	constant matrix
c	non-linear function of states
$\mathbf{C}$	constant matrix
e_{g}	global error
e_x	tracking error norm
e_{Φ}	parameter estimation error norm
$\boldsymbol{e}$	rotation tracking error
$\boldsymbol{e}_{\mathrm{f}}$	filtered tracking error
g	gravitational acceleration
I_1	mass moment of inertia of the shoulder link with respect to its centre of mass
I_2	mass moment of inertia of the elbow link with respect to its centre of mass
$\mathbf{K}_{\mathrm{v}}$, $\mathbf{K}_{\mathrm{p}}$	diagonal-control gain matrices
l_1	length of the shoulder link
l_2	length of the elbow link
l_{c1}	centre of mass of the shoulder link with respect to its joint
l_{c2}	centre of mass of the elbow link with respect to its joint
m_{a}	mass at the shoulder tip
m_{b}	mass at the elbow tip
m_1	mass of the shoulder link
m_2	mass of the elbow link
$\mathbf{M}$	inertia matrix
$\hat{\mathbf{M}}$	estimated inertia matrix
p_{h_i}	upper bounds of components of $\boldsymbol{P}$
p_{l_i}	lower bounds of components of $\boldsymbol{P}$
$\boldsymbol{P}$	robot unknown parameters
$\hat{\boldsymbol{P}}$	estimated robot parameters
$\boldsymbol{Q}$	centrifugal and Coriolis forces
$\hat{\boldsymbol{Q}}$	estimated centrifugal and Coriolis forces
$\mathbf{R}$	positive definite matrix
$\mathbf{R}_1$	positive definite matrix
t	time
$\mathbf{W}$	regressor matrix
$\boldsymbol{x}$	tracking error
y, z	robot task space coordinates
α	scalar
$\boldsymbol{\Gamma}$	control gain matrix
$\boldsymbol{\tau}$	joints control torque
$\boldsymbol{\varphi}$	rotation of the links
$\boldsymbol{\varphi}_{\mathrm{d}}$	desired rotation of the links
$\dot{\boldsymbol{\varphi}}$	angular velocity of the links
$\boldsymbol{\Psi}$	positive diagonal matrix
ω	manoeuvre frequency
$\boldsymbol{\Omega}$	positive definite matrix
$\boldsymbol{\Phi}$	parameters estimation error

The MS was received on 20 October 1997 and was accepted after revision for publication on 25 May 1999.
* *Corresponding author: Mechanical Engineering Department, University of Saskatchewan, 57 Campus Drive, Saskatoon, Saskatchewan, Canada S7N 5A9.*

1 INTRODUCTION

In the late 1980s, several globally convergent adaptive control schemes for rigid link manipulators appeared in the literature and were reviewed in reference [**1**]. These schemes belong to two distinct categories. The first category makes use of the adaptive inverse dynamics (or computed torque), while the second category preserves the passivity properties of the rigid manipulator system. Adaptive control laws may be classified on the basis of their control objective and the signal that drives the parameter update law. The update law can be driven by the signal that measures the prediction error (the error between the predicted torque and the torque required for the manipulator to follow the given path [**2**, **3**]) or by the signal that measures the tracking error (the error between the desired output and the plant output [**4**]).

The first category, the adaptive inverse dynamics approach, leads to a closed-loop system which is linear and decoupled. The research described in references [**4**] and [**5**] uses the adaptive inverse dynamics and the tracking error to drive the update law. The scheme used in reference [**4**] requires both the measurement of the joint acceleration and the boundedness of the inverse of the estimated inertia matrix. According to Spong and Ortega [**5**], their method does not require boundedness of the estimated inertia matrix. However, it was proved in reference [**6**] and admitted by Spong and Ortega [**5**] that the inverse of the estimated inertia-related matrix must be bounded for the acceleration to be bounded. Thus, the approach of reference [**5**] does not remove the requirement of the boundedness of the estimated inertia matrix imposed in reference [**4**]. Measurement of the joint acceleration, required in the regressor matrix, was later removed in reference [**2**] by using a first-order filter. The boundedness of the estimated inertia matrix was required there. In reference [**7**] the formulation of reference [**4**] was used with a different Lyapunov function. An interesting aspect of that paper was that it adapted the velocity control gain as if it was an unknown parameter. Also in reference [**8**], the formulation of reference [**4**] was used with one simplifying assumption that the inertia matrix was constant; therefore it did not require on-line calculation of the inversion of the matrix. However, this was not a realistic assumption as it was shown in reference [**8**] by simulation that the estimated parameters did not converge to their true values.

The second class of manipulator adaptive control, the passivity-based control approach, has been attractive since it leads in the adaptive controller to error equations where the regressor matrix is independent of the joint acceleration. The disadvantage of this scheme is that the closed-loop system remains non-linear and coupled. Sadegh and Horowitz [**9**] and Slotine and Li [**10**] used this type of adaptive controller. Although convergence of the trajectory tracking is guaranteed in reference [**10**], the estimated parameters do not necessarily converge to their true values as stated there. In fact, they did not converge to their true values because the desired trajectory was not persistently exciting [**10**]. Some experimental results using the same control law as used in reference [**10**] were given in reference [**11**], which used a direct adaptive controller and parameter adaptation driven by the tracking error. A trajectory following problem for a rigid links manipulator using an adaptive–robust controller was discussed in reference [**12**]. The only difference between the results discussed in that paper and existing results in the literature was that the unknown bounded functional dynamics were included in the equation of the manipulator. However, in the numerical results reported there, using the same adaptation law as in reference [**9**], the estimated parameters did not converge. The algorithm given in reference [**13**] also relied on the passivity property [**1**] and linear-in-parameters property [**14**] of the rigid manipulators. This was a modification of the work in reference [**10**] in which an error norm of parameter estimation was updated rather than the parameters themselves. The drawback of this work was that it did not guarantee that the estimated parameters converged to their true values as only their error norm was calculated on line. The results given in reference [**15**] were also based on the passivity-based control approach, which is an alternative way of reducing the sensitivity of velocity measurement to noise proposed by reference [**9**]. Defining too many bounds for the terms used in that paper beforehand and tuning several gains may make this approach difficult. The work in reference [**16**] was an extension of the work in reference [**9**] for repetitive and adaptive motion when the joint velocities cannot be measured by the control system. An observer was used to estimate the manipulator joint velocities with the assumption that the desired trajectory jerks are continuous and available. However, the simulation study reported was solely for repetitive (cyclic) motion. The work in reference [**17**] was also an extension of the work in reference [**9**] for a rigid link tracking adaptive controller using only joint position measurement. A filtering technique was used to compensate the need for the velocity measurements. The simulation results in reference [**17**], however, showed a large variation in the link position tracking error, which is not desirable. A proportional–derivative tracking controller with fixed gains (non-adaptive) for a robot manipulator was given in Paden and Panja [**18**]. They put the manipulator inertia matrix outside the position and velocity feedback loops.

The adaptive control strategy used in this paper is similar to that presented in references [**4**] and [**19**], but with a more complete mathematical dynamic model for two-link rigid manipulators (TLRMs). In particular, in deriving the dynamic equation of motion, all the physical parameters of the manipulators, including the distributed masses of the links, are taken into the account. Also, it is shown that, when the control gain matrix $\mathbf{\Gamma}$

is not constant, the convergence of the adaptation law will be increased. This is an important difference from the studies mentioned previously, where this gain was considered a known constant matrix. Measurement of the joint acceleration is required to ensure convergence of the adaptation law. Explicit expressions for a norm of the tracking error and for a norm of the parameter estimation error are given and calculated in the numerical simulation. It is shown that these error norms converge to zero in time smoothly. Also, the relation between the tracking error and the parameter estimation error is derived. This relation facilitates selection of the control parameters. In particular, the gains of the adaptive controller, $\mathbf{\Gamma}$, can be automatically calculated at the start of the process. In the simulation, an ellipse is considered as the desired trajectory which is to be followed by the tip of the TLRM. This scheme may also be used for multi-link rigid manipulators. A brief description of such applications was presented in reference [**3**].

2 STATEMENT OF THE PROBLEM

The TLRM shown in Fig. 1 can be modelled as a set of two rigid bodies connected in a serial chain with or without friction. The set (φ_1, φ_2) is chosen rather than the inertia set $(\theta_1 = \varphi_1, \theta_2 = \varphi_1 + \varphi_2)$ because it makes measurements of the rotation angles easier. Also, this set of coordinates is most common in the literature.

Similarly, as in reference [**19**], the equation of motion is obtained in the form

$$\mathbf{M}(\boldsymbol{\varphi}, \boldsymbol{P})\ddot{\boldsymbol{\varphi}}(t) + \boldsymbol{Q}(\boldsymbol{\varphi}, \dot{\boldsymbol{\varphi}}, \boldsymbol{P}) = \boldsymbol{\tau}(t) \tag{1}$$

where $\boldsymbol{Q}$ and $\mathbf{M}$ are vector and matrix non-linear functions of the degrees of freedom and a vector $\boldsymbol{P}$ of unknown parameters, $\boldsymbol{\tau}$ is the vector of controls represented by the torques τ_1 and τ_2, and $\boldsymbol{\varphi}$ is the vector of the degrees of freedom needed to define the motion and the trajectory of the manipulator. The first term, $\mathbf{M}\ddot{\boldsymbol{\varphi}}$, in equation (1) represents the inertia forces and the second term, $\boldsymbol{Q}$, includes the centrifugal and Coriolis effects and may include gravitational, friction and other forces. These two terms contain r system parameters $\boldsymbol{P} = [p_1\ p_2\ \cdots\ p_r]^{\mathrm{T}}$, which have to be estimated by the controller during the manoeuvre. The objective is that the manipulator follows a given trajectory specified by $\boldsymbol{\varphi}_{\mathrm{d}}$ and is controlled by a non-linear adaptive controller that is described in the following section.

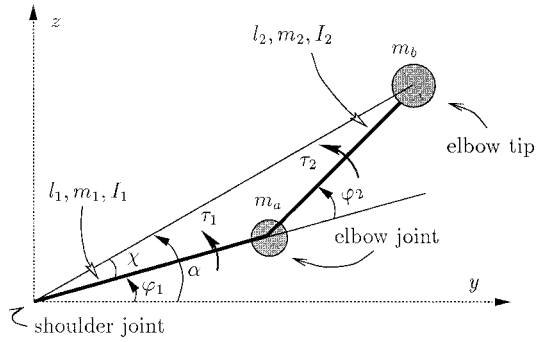

Fig. 1 Physical parameters used in the formulation of TLRMs

In this analysis, I_1 and I_2 are the mass moments of inertia of the links with respect to their centres of mass, m_1 and m_2 are the masses of the shoulder and the elbow links respectively, m_{a} is the mass at the elbow joint and m_{b} is the mass at the tip of the manipulator. The lengths of the links are l_1 and l_2, whereas l_{c1} and l_{c2} locate the centres of mass of the links. The states φ_1 and $\dot{\varphi}_1$ are the rotation and angular velocity respectively of the shoulder link, φ_2 and $\dot{\varphi}_2$ are the rotation and angular velocity respectively of the elbow link and g is the gravitational acceleration. The manipulator is driven by motors installed at the shoulder and elbow joints and generates the torques τ_1 and τ_2 respectively. The explicit form of the equations of motion is

$$\begin{aligned} &a_{11}\ddot{\varphi}_1 + a_{12}\ddot{\varphi}_2 - a_{13}(2\dot{\varphi}_1 + \dot{\varphi}_2)\dot{\varphi}_2 + a_{14}g = \tau_1(t) \\ &a_{12}\ddot{\varphi}_1 + a_{22}\ddot{\varphi}_2 + a_{13}\dot{\varphi}_1^2 + a_{24}g = \tau_2(t) \end{aligned} \tag{2}$$

where a_{ij} are known functions of the physical parameters and rotations φ_1 and φ_2. Details of this equation can be found in Appendix 2. In the form of equation (1), these equations are

$$\mathbf{M}(\boldsymbol{\varphi}, \boldsymbol{P}) = \begin{bmatrix} a_{11} & a_{12} \\ a_{12} & a_{22} \end{bmatrix}$$

$$\boldsymbol{Q}(\boldsymbol{\varphi}, \dot{\boldsymbol{\varphi}}, \boldsymbol{P}) = \begin{Bmatrix} -a_{13}(2\dot{\varphi}_1 + \dot{\varphi}_2)\dot{\varphi}_2 + a_{14}g \\ +a_{13}\dot{\varphi}_1^2 + a_{24}g \end{Bmatrix}$$

This TLRM using an adaptive algorithm described here was simulated and is discussed in Section 4.

3 ADAPTIVE CONTROL OF TWO-LINK RIGID MANIPULATORS

To control the motion of the TLRM so as to follow a given path a model-based adaptive controller was developed as discussed in the following (Fig. 2).

3.1 Model-based control

The tracking error indicating how well the manipulator follows the desired trajectory is defined by

$$\boldsymbol{e}(t) = [e_1 \quad e_2]^{\mathrm{T}} = \boldsymbol{\varphi}_{\mathrm{d}} - \boldsymbol{\varphi} \tag{3}$$

The desired trajectory of the manipulator is described by $\boldsymbol{\varphi}_{\mathrm{d}}(t)$, $\dot{\boldsymbol{\varphi}}_{\mathrm{d}}(t)$ and $\ddot{\boldsymbol{\varphi}}_{\mathrm{d}}(t)$, which are assumed to be given functions of time.

The r unknown system parameters are estimated by $\hat{\boldsymbol{P}} = [\hat{p}_1\ \hat{p}_2\ \cdots\ \hat{p}_r]^{\mathrm{T}}$ and the parameters estimation error

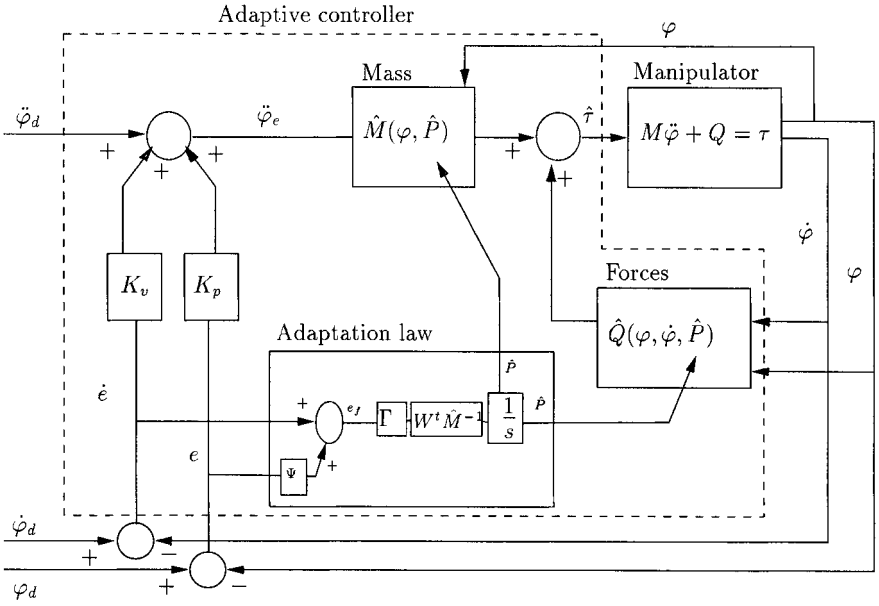

Fig. 2 Adaptive controller

vector is defined as

$$\boldsymbol{\Phi}(t) = \boldsymbol{P} - \hat{\boldsymbol{P}} \tag{4}$$

It is assumed, as in reference [**19**], that the system with the estimated parameters $\hat{\boldsymbol{P}}$ is driven by the following control law:

$$\boldsymbol{\tau}(t) = \mathbf{M}(\boldsymbol{\varphi}, \hat{\boldsymbol{P}})\ddot{\boldsymbol{\varphi}}_e + \boldsymbol{Q}(\boldsymbol{\varphi}, \dot{\boldsymbol{\varphi}}, \hat{\boldsymbol{P}}) \tag{5}$$

where $\mathbf{M}(\boldsymbol{\varphi}, \hat{\boldsymbol{P}})$ and $\boldsymbol{Q}(\boldsymbol{\varphi}, \dot{\boldsymbol{\varphi}}, \hat{\boldsymbol{P}})$ are estimates of $\mathbf{M}(\boldsymbol{\varphi}, \boldsymbol{P})$ and $\boldsymbol{Q}(\boldsymbol{\varphi}, \dot{\boldsymbol{\varphi}}, \boldsymbol{P})$ and

$$\ddot{\boldsymbol{\varphi}}_e(t) = \ddot{\boldsymbol{\varphi}}_d + \mathbf{K}_v\dot{\boldsymbol{e}} + \mathbf{K}_p\boldsymbol{e} \tag{6}$$

and $\mathbf{K}_v$ and $\mathbf{K}_p$ are 2×2 constant diagonal-gain matrices with k_{vj} and k_{pj} on the diagonals. The term, $\ddot{\boldsymbol{\varphi}}_e$, defines an acceleration modified in terms of the tracking error. This acceleration is then passed through equation (5) to provide the control torque $\boldsymbol{\tau}$. Equation (5) is sometimes referred to as the *computed torque method* [**20**] of manipulator control. Clearly, the torques determined by equation (5), when applied to the system governed by equation (1), will cause the manipulator to follow the desired trajectory only if the trajectory error $\boldsymbol{e}(t)$ and parameters estimation error $\boldsymbol{\Phi}(t)$ are zero. The adaptive controller observes the tracking error, adjusts the parameters $\hat{\boldsymbol{P}}$ and determines the torque vector $\hat{\boldsymbol{\tau}}$ according to the control law (5).

The relation between the tracking error $\boldsymbol{e}$ and the parameter estimation error $\boldsymbol{\Phi}$ can be obtained by equating (1) and (5), giving

$$\ddot{\boldsymbol{e}}(t) + \mathbf{K}_v\dot{\boldsymbol{e}}(t) + \mathbf{K}_p\boldsymbol{e}(t) = \hat{\mathbf{M}}^{-1}(\Delta\mathbf{M}\,\ddot{\boldsymbol{\varphi}} + \Delta\boldsymbol{Q}) \tag{7}$$

where

$$\hat{\mathbf{M}} = \mathbf{M}(\boldsymbol{\varphi}, \hat{\boldsymbol{P}}), \qquad \hat{\boldsymbol{Q}} = \boldsymbol{Q}(\boldsymbol{\varphi}, \dot{\boldsymbol{\varphi}}, \hat{\boldsymbol{P}})$$

and

$$\Delta\mathbf{M} = \mathbf{M} - \hat{\mathbf{M}}, \qquad \Delta\boldsymbol{Q} = \boldsymbol{Q} - \hat{\boldsymbol{Q}}$$

are errors in the dynamic model arising from errors in the parameters estimation of the model [see equation (4)].

Expanding $\mathbf{M}$ and $\boldsymbol{Q}$ into the Taylor series with respect to parameters $\boldsymbol{P}$ and considering only the linear terms gives

$$\mathbf{M}(\boldsymbol{\varphi}, \boldsymbol{P}) \approx \mathbf{M}(\boldsymbol{\varphi}, \hat{\boldsymbol{P}}) + \frac{\partial\hat{\mathbf{M}}}{\partial\hat{\boldsymbol{P}}}\boldsymbol{\Phi} \tag{8}$$

$$\boldsymbol{Q}(\boldsymbol{\varphi}, \dot{\boldsymbol{\varphi}}, \boldsymbol{P}) \approx \boldsymbol{Q}(\boldsymbol{\varphi}, \dot{\boldsymbol{\varphi}}, \hat{\boldsymbol{P}}) + \frac{\partial\hat{\boldsymbol{Q}}}{\partial\hat{\boldsymbol{P}}}\boldsymbol{\Phi} \tag{9}$$

The tracking error equation (7) can be written now in the form

$$\ddot{\boldsymbol{e}}(t) + \mathbf{K}_v\dot{\boldsymbol{e}}(t) + \mathbf{K}_p\boldsymbol{e}(t) = \hat{\mathbf{M}}^{-1}\mathbf{W}(\boldsymbol{\varphi}, \dot{\boldsymbol{\varphi}}, \ddot{\boldsymbol{\varphi}}, \hat{\boldsymbol{P}})\boldsymbol{\Phi} \tag{10}$$

where $\mathbf{W}(\boldsymbol{\varphi}, \dot{\boldsymbol{\varphi}}, \ddot{\boldsymbol{\varphi}}, \hat{\boldsymbol{P}})$ is a $2 \times r$ regressor matrix defined as

$$\mathbf{W}(\boldsymbol{\varphi}, \dot{\boldsymbol{\varphi}}, \ddot{\boldsymbol{\varphi}}, \hat{\boldsymbol{P}}) = \frac{\partial\hat{\mathbf{M}}}{\partial\hat{\boldsymbol{P}}}\ddot{\boldsymbol{\varphi}} + \frac{\partial\hat{\boldsymbol{Q}}}{\partial\hat{\boldsymbol{P}}} \tag{11}$$

This matrix represents the sensitivity of the system to the parameters being identified. If the terms $\mathbf{M}$ and $\boldsymbol{Q}$ are linear functions of the system parameters $\boldsymbol{P}$, then equations (8) and (9) become exact and the left-hand side of equation (11) becomes independent of $\hat{\boldsymbol{P}}$. This then implies that

$$\mathbf{W}(\boldsymbol{\varphi}, \dot{\boldsymbol{\varphi}}, \ddot{\boldsymbol{\varphi}})\boldsymbol{\Phi} = \left(\frac{\partial\hat{\mathbf{M}}}{\partial\hat{\boldsymbol{P}}}\ddot{\boldsymbol{\varphi}} + \frac{\partial\hat{\boldsymbol{Q}}}{\partial\hat{\boldsymbol{P}}}\right)\boldsymbol{\Phi} = \Delta\mathbf{M}\,\ddot{\boldsymbol{\varphi}} + \Delta\boldsymbol{Q} \tag{12}$$

Essentially all parameters related to the manipulator's mass satisfy the above linear properties. Some parameters such as those representing dimensions of the links, or the location of the masses, can be converted into a linear form as explained in Appendix 2.

Considering equation (10), it is important that the product $\hat{\mathbf{M}}^{-1}\mathbf{W}$ remains bounded at all times. Since $\mathbf{W}$ is composed of bounded functions of the manipulator trajectory, it will remain bounded if the trajectory remains bounded. The matrix $\hat{\mathbf{M}}$ will remain positive definite and invertible if it is ensured that all the parameters in $\hat{\mathbf{M}}$ remain within the vicinity of the actual parameter value. For this, the estimated parameters should lie in the space

$$p_{l_i} - \delta < \hat{p}_i < p_{h_i} + \delta \tag{13}$$

where p_{l_i} and p_{h_i} are the lower and upper bounds respectively of the unknown parameters and δ is a positive number chosen to ensure that $\hat{\mathbf{M}}^{-1}$ remains bounded.

3.2 Adaption algorithm

The adaptive law determines how the system parameters are to be adjusted as a function of the filtered tracking error signal. This filtered tracking error is

$$\boldsymbol{e}_f(t) = \dot{\boldsymbol{e}} + \boldsymbol{\Psi e} \tag{14}$$

where $\boldsymbol{\Psi}$ is a diagonal matrix with positive constants ψ_1 and ψ_2 on its diagonal.

The tracking error equation (10) and the filtered error equation (14) are written in the state space form as

$$\dot{\boldsymbol{x}}(t) = \mathbf{A}\boldsymbol{x} + \mathbf{B}\hat{\mathbf{M}}^{-1}\mathbf{W}\boldsymbol{\Phi} \tag{15}$$

$$\boldsymbol{e}_f(t) = \mathbf{C}\boldsymbol{x} \tag{16}$$

For a system with two degrees of freedom, such as a TLRM, there are four state variables defining the position and velocity errors for each link as follows:

$$\boldsymbol{x} = [e_1 \quad \dot{e}_1 \quad e_2 \quad \dot{e}_2]^T$$

In equations (15) and (16) the matrices $\mathbf{A}$, $\mathbf{B}$ and $\mathbf{C}$ are defined as

$$\mathbf{A} = \begin{bmatrix} 0 & 1 & 0 & 0 \\ -k_{p1} & -k_{v1} & 0 & 0 \\ 0 & 0 & 0 & 1 \\ 0 & 0 & -k_{p2} & -k_{v2} \end{bmatrix}$$

$$\mathbf{B} = \begin{bmatrix} 0 & 0 \\ 1 & 0 \\ 0 & 0 \\ 0 & 1 \end{bmatrix}$$

$$\mathbf{C} = \begin{bmatrix} \psi_1 & 1 & 0 & 0 \\ 0 & 0 & \psi_2 & 1 \end{bmatrix}$$

3.3 Convergence of the control process

The convergence of the control process is determined by monitoring the global error e_g:

$$e_g(t) = \boldsymbol{x}^T\boldsymbol{\Omega x} + \boldsymbol{\Phi}^T\boldsymbol{\Gamma}^{-1}\boldsymbol{\Phi} \tag{17}$$

where $\boldsymbol{\Omega}$ and $\boldsymbol{\Gamma}$ are symmetric positive definite matrices. The global error e_g is reduced to zero in time only if $\boldsymbol{x} \to 0$ and $\boldsymbol{\Phi} \to 0$. This error consists of two components: $e_x(t) = \boldsymbol{x}^T\boldsymbol{\Omega x}$, a norm representing the tracking error, and $e_{\boldsymbol{\Phi}}(t) = \boldsymbol{\Phi}^T\boldsymbol{\Gamma}^{-1}\boldsymbol{\Phi}$, a norm representing the parameter estimation error.

The convergence rate is determined by differentiating equation (17) with respect to time:

$$\dot{e}_g(t) = \boldsymbol{x}^T(\mathbf{A}^T\boldsymbol{\Omega} + \boldsymbol{\Omega}\mathbf{A})\boldsymbol{x} + 2\boldsymbol{\Phi}^T(\mathbf{W}^T\hat{\mathbf{M}}^{-1}\mathbf{B}^T\boldsymbol{\Omega x} + \boldsymbol{\Gamma}^{-1}\dot{\boldsymbol{\Phi}}) + \boldsymbol{\Phi}^T(\boldsymbol{\Gamma}^{-1})^{\bullet}\boldsymbol{\Phi} \tag{18}$$

Assuming that

$$\boldsymbol{\Omega B} = \mathbf{C}^T \tag{19}$$

and using equation (16) the second term in equation (18) disappears when

$$\dot{\boldsymbol{\Phi}}(t) = -\boldsymbol{\Gamma}\mathbf{W}^T\hat{\mathbf{M}}^{-1}\boldsymbol{e}_f \tag{20}$$

To facilitate the choice of $\boldsymbol{\Omega}$ assume that

$$\mathbf{A}^T\boldsymbol{\Omega} + \boldsymbol{\Omega}\mathbf{A} = -\mathbf{R} \tag{21}$$

where $\mathbf{R}$ is a positive definite matrix. Substituting equations (20) and (21) into equation (18) results in

$$\dot{e}_g(t) = -\boldsymbol{x}^T\mathbf{R}\boldsymbol{x} + \boldsymbol{\Phi}^T(\boldsymbol{\Gamma}^{-1})^{\bullet}\boldsymbol{\Phi} \tag{22}$$

If $\boldsymbol{\Gamma}$ is assumed constant, then only a positive definite $\mathbf{R}$ is required for the global error $e_g(t)$ to decrease monotonically in time. Such a case was considered in reference [**19**] when Lyapunov theory was used in the stability analysis. The convergence rate may be faster if also $(\boldsymbol{\Gamma}^{-1})^{\bullet}$ is negative definite. Note that based on the Kalman–Yakubovich lemma [**14**], positive definite matrices $\boldsymbol{\Omega}$ and $\mathbf{R}$ exist.

The symmetric matrix $\boldsymbol{\Omega}$, according to equation (19), must have the form

$$\boldsymbol{\Omega} = \begin{bmatrix} \Omega_{11} & \psi_1 & \Omega_{13} & 0 \\ \psi_1 & 1 & 0 & 0 \\ \Omega_{13} & 0 & \Omega_{33} & \psi_2 \\ 0 & 0 & \psi_2 & 1 \end{bmatrix} \tag{23}$$

Substituting equation (23) into equation (21) gives

$$\mathbf{R} = \begin{bmatrix} 2k_{p1}\psi_1 & k_{p1} + \psi_1 k_{v1} - \Omega_{11} & 0 & -\Omega_{13} \\ & 2(k_{v1} - \psi_1) & -\Omega_{13} & 0 \\ & & 2k_{p2}\psi_2 & k_{p2} + \psi_2 k_{v2} - \Omega_{33} \\ \text{symmetric} & & & 2(k_{v2} - \psi_2) \end{bmatrix} \tag{24}$$

The remaining components of $\mathbf{\Omega}$ can be determined by requesting that the matrix $\mathbf{R}$ be diagonal:

$$\Omega_{11} = k_{p1} + \psi_1 k_{v1}, \qquad \Omega_{33} = k_{p2} + \psi_2 k_{v2}, \qquad \Omega_{13} = 0 \tag{25}$$

Substituting equation (25) into equation (24) the diagonal elements of matrix $\mathbf{R}$ are obtained as

$$r_{11} = 2k_{p1}\psi_1, \qquad r_{22} = 2(k_{v1} - \psi_1)$$
$$r_{33} = 2k_{p2}\psi_2, \qquad r_{44} = 2(k_{v2} - \psi_2) \tag{26}$$

Now, for $\mathbf{R}$ to be positive definite, the following is required:

$$k_{vj} > \psi_j > 0, \qquad j = 1, 2 \tag{27}$$

Additionally, it can be assumed that the convergence level for the tracking position error e_j and the tracking velocity error $\dot{e}_j$ are similar if the corresponding diagonal terms in $\mathbf{R}$ are set equal, i.e. $r_{11} = r_{22} = 2r_1$, $r_{33} = r_{44} = 2r_2$, where

$$r_j = k_{pj}\psi_j = k_{vj} - \psi_j, \qquad j = 1, 2 \tag{28}$$

This implies the following choice for $\mathbf{\Psi}$:

$$\psi_j = \frac{k_{vj}}{1 + k_{pj}}, \qquad j = 1, 2 \tag{29}$$

Using equation (25) in equation (23) the matrix $\mathbf{\Omega}$ is uniquely defined as

$$\mathbf{\Omega} = \begin{bmatrix} k_{p1} + \psi_1 k_{v1} & \psi_1 & 0 & 0 \\ & 1 & 0 & 0 \\ & & k_{p2} + \psi_2 k_{v2} & \psi_2 \\ \text{symmetric} & & & 1 \end{bmatrix} \tag{30}$$

Note that, with equation (29), $\mathbf{\Omega}$ is always positive definite. One can verify that $k_{p1} + \psi_1 k_{v1} > \psi_1^2$ and $k_{p2} + \psi_2 k_{v2} > \psi_2^2$.

It should be noted that the transfer function of the filtered error $\boldsymbol{e}_f = G(s)(\hat{\mathbf{M}}^{-1}\mathbf{W}\boldsymbol{\Phi})$, $G(s) = (s + \psi_j)/(s^2 + k_{vj}s + k_{pj})$, derived from equations (15) and (16), is strictly positive real (SPR) because

$$\mathrm{Re}[G(\mathrm{j}\omega)] = \mathrm{Re}[(\mathrm{i}\omega + \psi_j)(-\omega^2 - k_{vj}\mathrm{i}\omega + k_{pj})]$$
$$= (k_{vj} - \psi_j)\omega^2 + \psi_j k_{pj} > 0, \qquad \forall \omega \geqslant 0$$

due to equation (29). This means that the phase shift of $G(s)$ must always have a magnitude of 90° or less in response to sinusoidal inputs, and $G(s)$ is strictly minimum phase, i.e. all its zeros are strictly in the left-half plane [**14**].

Using equations (4) and (20), the *adaptation law* reduces to

$$\dot{\hat{\boldsymbol{P}}}(t) = \mathbf{\Gamma}\mathbf{W}^{\mathrm{T}}\hat{\mathbf{M}}^{-1}\boldsymbol{e}_f \tag{31}$$

It is assumed that $\mathbf{\Gamma}$ is a diagonal matrix with positive elements $(\gamma_1, \gamma_2, \ldots, \gamma_r)$ on its diagonal. This law is identical with that derived in reference [**19**], where $\mathbf{\Gamma}$ can be considered as a gain matrix for parameter identification. Using the reset conditions (13) the update law is augmented as

$$\hat{p}_i(t^+) = p_{l_i} \qquad \text{if } \hat{p}_i(t) \leqslant p_{l_i} - \delta \tag{32}$$

$$\hat{p}_i(t^+) = p_{h_i} \qquad \text{if } \hat{p}_i(t) \geqslant p_{h_i} + \delta \tag{33}$$

Equations (17) and (22) imply that $\boldsymbol{x}$ and $\boldsymbol{\Phi}$ are bounded. The addition of parameter resetting maintains the non-positiveness of $\dot{e}_g(t)$ and the system remains stable even when $\boldsymbol{x}$ and $\boldsymbol{\Phi}$ are bounded.

According to equation (22) for $\mathbf{\Gamma} = \mathbf{\Gamma}_0$ constant and for $\mathbf{R}$ positive definite, the global error will decrease for any value of the tracking error until $\boldsymbol{x} \to \mathbf{0}$. However, if $\boldsymbol{x} \to \mathbf{0}$, then $\boldsymbol{e}_f \to \mathbf{0}$ [see equation (16)] and $\dot{\hat{\boldsymbol{\Phi}}} \to \mathbf{0}$ [see equation (20)]. If, additionally, $\dot{\boldsymbol{x}} \to \mathbf{0}$, then $\boldsymbol{\Phi} \to \mathbf{0}$ [see equation (15)] and the system parameters are identified properly.

The convergence may be improved if $(\mathbf{\Gamma}^{-1})^{\bullet}$ is also negative definite. For example, the following alternative may be considered:

$$(\mathbf{\Gamma}^{-1})^{\bullet} = -\mathbf{\Gamma}^{-1}\dot{\mathbf{\Gamma}}\mathbf{\Gamma}^{-1} < 0$$
$$\dot{\mathbf{\Gamma}}(t) = \alpha\, \mathrm{e}^{-\alpha t}\mathbf{R}_1 > 0$$
$$\mathbf{\Gamma}(t) = \mathbf{\Gamma}_0 + (1 - \mathrm{e}^{-\alpha t})\mathbf{R}_1 \tag{34}$$

where $\mathbf{R}_1$ and α are a positive definite diagonal matrix and a scalar respectively and $\mathbf{\Gamma}_0$ is the constant matrix defined earlier.

To start the simulation the values of the gain matrices $\mathbf{K}_v$ and $\mathbf{K}_p$ are assumed. Then the values of $\mathbf{\Psi}$, $\mathbf{R}$ and $\mathbf{\Omega}$ are obtained from equations (29), (28) and (30) respectively. Note that, if the matrix $\mathbf{\Omega}$ is known, the tracking error norm e_x can be calculated. Normally, the elements of diagonal matrix $\mathbf{\Gamma}$ that are required to determine the estimation error norm e_{Φ} are assumed independently. However, the sets of parameters in $\mathbf{\Gamma}$ and $\mathbf{\Omega}$ can be related to one another by making the error norms e_x and e_{Φ} as similar as possible. This idea is presented in Appendix 1 although, in the examples presented, the final choice of the values of $\mathbf{\Gamma}$ and $\mathbf{\Omega}$ was found mainly by the numerical experimentation.

4 SIMULATION RESULTS

Using the adaptive control algorithm derived in Section 3, simulation studies of the TLRM shown in Fig. 1 were carried out, and the case where the controller must estimate the parameters $m_a = p_1$ and $m_b = p_2$ will now be considered. Since **M** and $\boldsymbol{Q}$ are linearly dependent on these two parameters, equations (8) and (9) are exact, and the matrix **W** for $r = 2$ is defined as

$$\mathbf{W}_{2\times 2} = \begin{bmatrix} w_{11} & w_{12} \\ 0 & w_{22} \end{bmatrix} \tag{35}$$

where details of w_{ij} can be found in Appendix 2.

4.1 Following a given elliptical trajectory

In this particular example, the desired trajectory is defined in the form of an ellipse with the centre coordinates $y_0 = 0.5$ m, $z_0 = 0.5$ m and $\theta = 45^\circ$ rotation with respect to the y axis, and the manoeuvre frequency was $\omega = 0.5$ rad/s (the period was 4π s). The principal diameters of the ellipse were respectively $a = 0.5$ m and $b = 0.23$ m.

The trajectory can be parametrized as (see Fig. 1)

$$\begin{aligned} y_1(t) &= a\cos(\omega t) \\ z_1(t) &= b\sin(\omega t) \\ y_2(t) &= y_1\cos(\theta) - z_1\sin(\theta) \\ z_2(t) &= y_1\sin(\theta) + z_1\cos(\theta) \\ y(t) &= y_0 + y_2 \\ z(t) &= z_0 + z_2 \end{aligned} \tag{36}$$

The rotation angles of the manipulator are

$$\begin{aligned} \varphi_1(t) &= \alpha - \chi \\ \chi(t) &= \cos^{-1}\left(\frac{y^2 + z^2 + l_1^2 - l_2^2}{2l_1\sqrt{y^2 + z^2}}\right) \\ \alpha(t) &= \tan^{-1}\left(\frac{z}{y}\right) \\ \varphi_2(t) &= \cos^{-1}\left(\frac{y^2 + z^2 - l_1^2 - l_2^2}{2l_1 l_2}\right) \end{aligned}$$

For simulation purposes the physical parameters of the manipulator and control gains were set to

$$\begin{aligned} &l_1 = 2l_{c1} = 1 \text{ m}\ , \quad m_a = 4 \text{ kg}, \quad g = 9.81 \text{ m/s}^2 \\ &l_2 = 2l_{c2} = 1 \text{ m}\ , \quad m_b = 2 \text{ kg}, \quad I_1 = 0 = I_2 \\ &k_{v1} = 30 = k_{v2}\ , \quad m_1 = 0 \\ &k_{p1} = 225 = k_{p2}, \quad m_2 = 0 \end{aligned} \tag{37}$$

4.2 Case 1: identification process of estimated parameters

Figures 3 to 10 show some of the simulation results which started with the following initial values for parameters estimation:

$$\hat{p}_1 = \hat{m}_a = 3, \qquad \hat{p}_2 = \hat{m}_b = 1.5$$

The lower and upper bounds of the parameters in

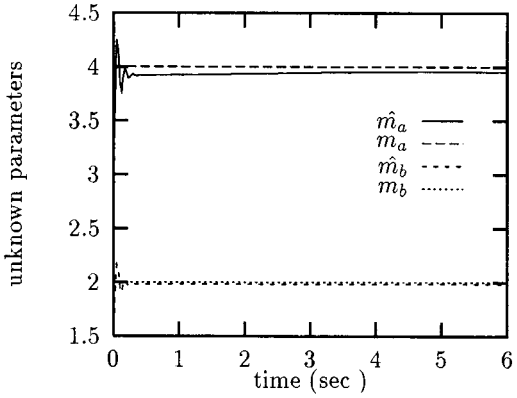

Fig. 3 Convergence of the estimated parameters with $\gamma_1 = 400$ and $\gamma_2 = 180$ for case 1

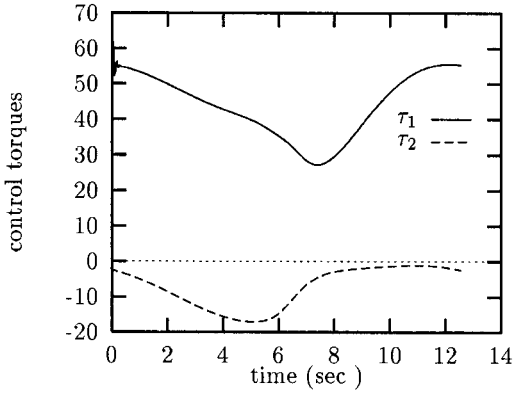

Fig. 4 Adaptive control torques with $\gamma_1 = 400$ and $\gamma_2 = 180$ for case 1

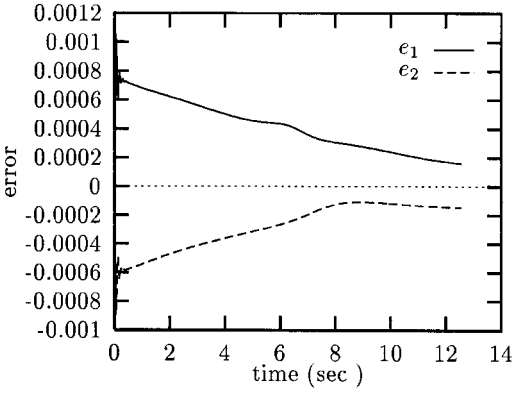

Fig. 5 Convergence of the tracking error of the rotations with $\gamma_1 = 400$ and $\gamma_2 = 180$ for case 1

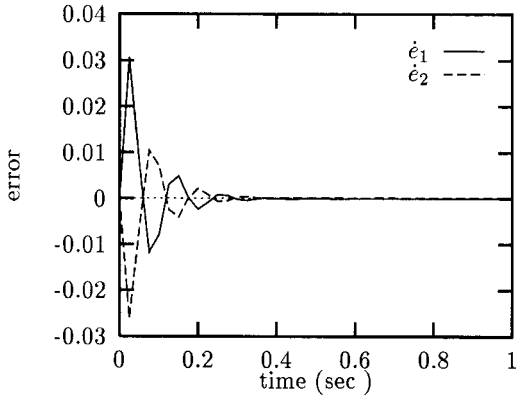

Fig. 6 Convergence of the tracking error of the angular velocities with $\gamma_1 = 400$ and $\gamma_2 = 180$ for case 1

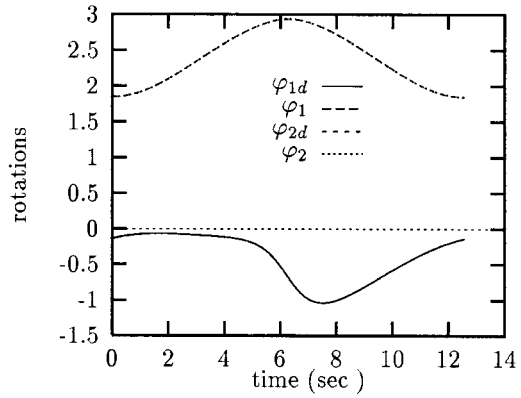

Fig. 7 Rotations of the links for the desired and calculated paths with $\gamma_1 = 400$ and $\gamma_2 = 180$ for case 1

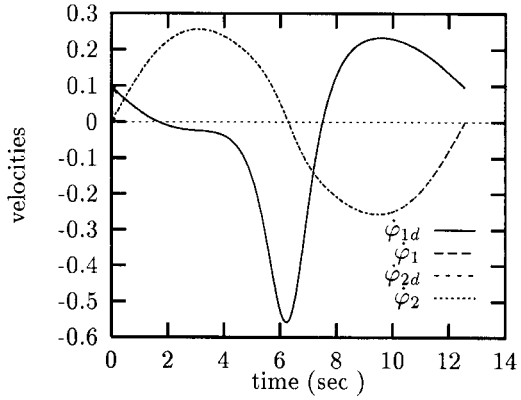

Fig. 8 Angular velocities of the links for the desired and calculated paths with $\gamma_1 = 400$ and $\gamma_2 = 180$ for case 1

equations (32) and (33) were set as $p_{l_1} = 2.0$, $p_{h_1} = 6.0$, $p_{l_2} = 1.0$, $p_{h_2} = 3.0$ and $\delta = 0.1$. The limit for the parameters variations were $1.9 \leqslant \hat{m}_a \leqslant 6.1$ and $0.9 \leqslant \hat{m}_b \leqslant 3.1$. Figure 3 shows how the unknown parameters $\hat{m}_a$ and $\hat{m}_b$ converged to their true values when $\gamma_1 = 400$ and $\gamma_2 = 180$. After about 0.5 s the estimated parameters had converged, or become close to the real parameters. This time was about 25 times smaller than the total manoeuvre time which is $t_f = 4\pi = 12.57$ s.

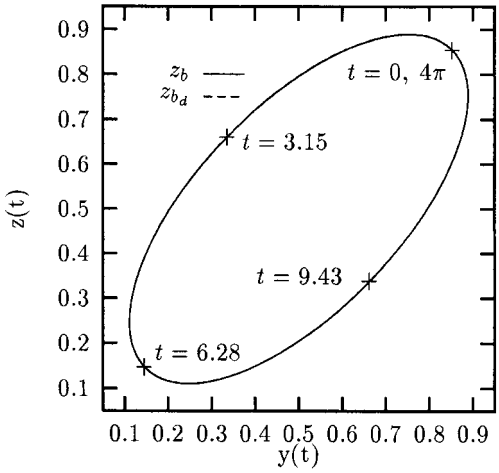

Fig. 9 Desired (z_{bd}) and calculated (z_b) trajectories (yz plane) with $\gamma_1 = 400$ and $\gamma_2 = 180$ for case 1

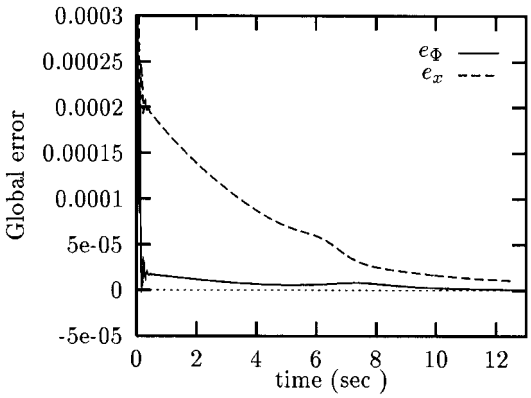

Fig. 10 Convergence of the components of the global error, $e_{\boldsymbol{\Phi}}$ and e_x, with $\gamma_1 = 400$ and $\gamma_2 = 180$ for case 1

As can be seen from Fig. 9, during the identification process the tip of the manipulator followed the desired path during and at the completion of the identification process. The deviation of the tip of the manipulator from the prescribed path was almost zero. Figure 4 shows the computed adaptive control torques as functions of time corresponding to Fig. 3. These were the torques that caused the tip of the manipulator to follow the desired elliptical trajectory. Figure 5 shows the errors in the tracking rotations of the links ($e_1 = \varphi_{1d} - \varphi_1$ and $e_2 = \varphi_{2d} - \varphi_2$). It can be concluded from this figure and Fig. 3 that, when the unknown parameters of the system are identified, both the tracking error $\boldsymbol{x}(t)$ and the parameters error $\boldsymbol{\Phi}(t)$ approach zero. The same argument holds for Fig. 6. Figure 6 shows the errors in the tracking velocities of the links ($\dot{e}_1 = \dot{\varphi}_{1d} - \dot{\varphi}_1$ and $\dot{e}_2 = \dot{\varphi}_{2d} - \dot{\varphi}_2$). Figure 7 shows the rotations of the links for the desired and calculated paths. As shown, the prescribed and calculated rotations were very similar as they almost coincide on the plot. Figure 8 shows the angular velocities of the links for the desired and calculated paths. They also coincide on the plot. Figure 9 shows the desired and

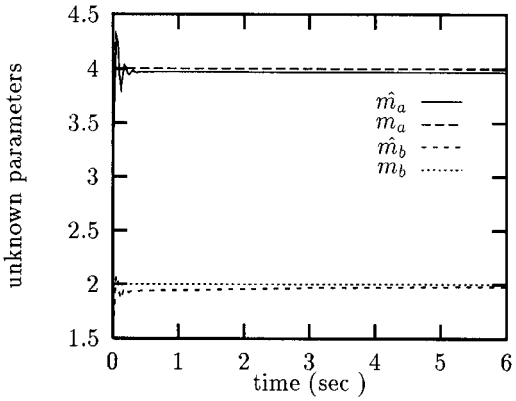

Fig. 11 Convergence of the estimated parameters with $\gamma_1 = 400$ and $\gamma_2 = 150$ for case 2

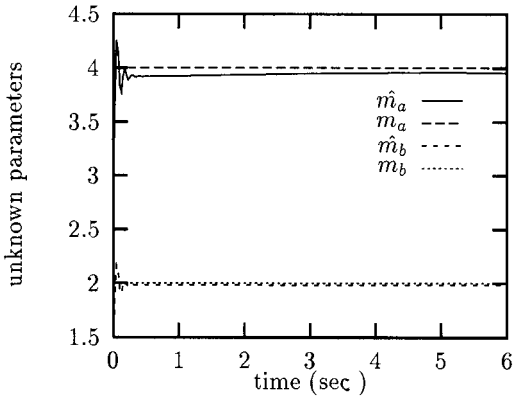

Fig. 12 Convergence of the estimated parameters with $\gamma_1(0) = 400$ and $\gamma_2(0) = 180$ for case 3

calculated trajectories in the yz plane for $0 \leqslant t \leqslant 4\pi$ for the identification process corresponding to Fig. 3. These plots also coincide in Fig. 9. Figure 10 shows the convergence of the components of the global error

$$e_g(t) = e_x + e_{\Phi} \tag{38}$$

in time with $\gamma_1 = 400$ and $\gamma_2 = 180$.

4.3 Case 2: effects of the matrix Γ on convergence

The matrix $\boldsymbol{\Gamma}$ plays an important role in the adaptation law (31). A good choice for γ_i may cause a rapid convergence of the unknown parameters $\hat{\boldsymbol{P}}$ to their true values, and a poor choice may have the converse effects. In this case, this parameter was considered constant in time. To see the effect of $\boldsymbol{\Gamma}$, the identification process presented in Fig. 3 was repeated with different values of γ_i. The results shown in Fig. 11 are similar to those in Fig. 3 where the parameter $\gamma_2 = 180$ was replaced by $\gamma_2 = 150$, which caused the convergence of $\hat{m}_b$ to a value lower than its true value. As in Fig. 3, the time needed for the estimated parameters to come close to the real values was about 12 times smaller than the total manoeuvre time.

4.4 Case 3: matrix Γ as a function of time

When the matrix $\boldsymbol{\Gamma}$ is an exponential function of time, as defined in equation (34), then $(\boldsymbol{\Gamma}^{-1})^{\bullet}$ is also negative definite and the convergence of the components of the norm of parameter estimation error, e_{Φ}, may be improved as discussed earlier. To implement this part for case 1, the following set of data was chosen:

$$\alpha = 0.5, \qquad \mathbf{R}_1 = \begin{bmatrix} 400 & 0 \\ 0 & 120 \end{bmatrix}$$

$$\gamma_1(0) = 400, \qquad \gamma_2(0) = 180$$

$$\gamma_1^{\max} = 800, \qquad \gamma_2^{\max} = 300$$

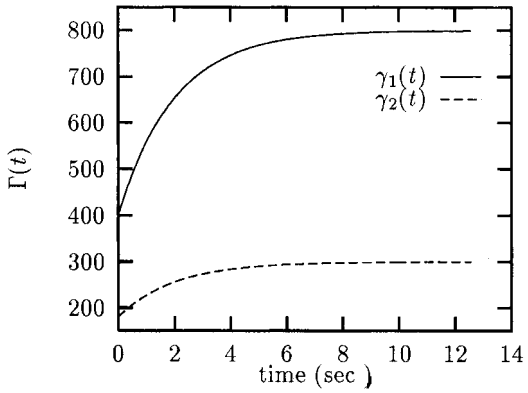

Fig. 13 Components of the gain matrix $\boldsymbol{\Gamma}(t)$ with $\gamma_1(0) = 400$ and $\gamma_2(0) = 180$ for case 3

where $\gamma_i^{\max}$ are the saturation limits of components of the gain matrix $\boldsymbol{\Gamma}$.

Figures 12 and 13 are the results of this implementation. Figure 12 shows how the unknown parameters $\hat{m}_a$ and $\hat{m}_b$ converge to their true values. As in Fig. 3, the time needed for the estimated parameters to come close to the real values was about ten times smaller than the total manoeuvre time. Figure 13 shows the gain matrix $\boldsymbol{\Gamma}(t)$ as an exponential function of time. As seen, they increased sharply in time and caused $e_{\Phi}(t)$ to decrease faster than the constant gain $\boldsymbol{\Gamma}$.

4.5 Case 4: adaptation process of estimated parameters

In this section, *identification* is referred to as that process which identifies the unknown parameters for the first time. After the identification process is completed, the unknown parameters $\hat{\boldsymbol{P}}$ are estimated. The adaptation process refers to those situations where the real values of the unknown parameters $\boldsymbol{P}$ were changed during the manoeuvre. In other words, some of the system parameters become unknown during the manoeuvre while they might be known initially. In the simulation studies of this case, step changes in m_a and m_b were assumed.

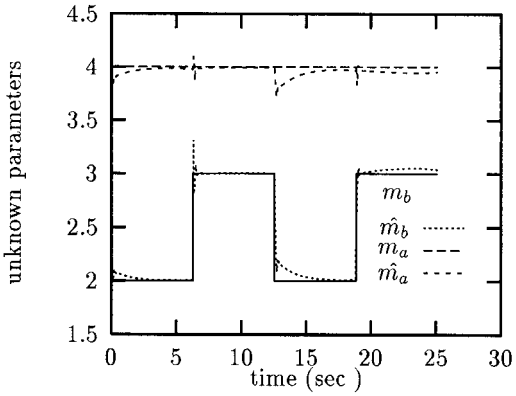

Fig. 14 Adaptation of the estimated parameters with change in m_b with $\gamma_1 = 2000$ and $\gamma_2 = 2500$ for case 4

As shown in Fig. 14, the estimated parameters were set to

$$\hat{m}_a = 4, \qquad \hat{m}_b = 2.5$$

initially, and the mass at the tip of manipulator changed from $m_b = 2$ to $m_b = 3.0$ alternatively at each half-cycle of the elliptical trajectory, i.e. at $t = 0.0$, $t = 6.28$, $t = 12.56$, $t = 18.85$ with $\gamma_1 = 2000$ and $\gamma_2 = 2500$. This figure clearly indicates that the adaptation law resulted in the convergence of the unknown parameter $\hat{m}_b$ to its new value in a fraction of a second. The unknown parameter $\hat{m}_a$ converged again to its true value after a disturbance due to the change in m_b. The desired and calculated trajectories in the yz plane for $0 \leqslant t \leqslant 4\pi$ for the adaptation process due to this change in m_b were the same as in Fig. 9.

In Fig. 15, the estimated parameters were known initially, and the mass at the elbow joint was changed from $m_a = 4$ to $m_a = 4.5$ at $t = 2$ with $\gamma_1 = 800$ and $\gamma_2 = 200$. This figure shows that the convergence of the unknown parameter $\hat{m}_a$ to its new value occurs in a fraction of a second. The unknown parameter $\hat{m}_b$ also converged to its true value shortly after the disturbance due to the change in m_a. The desired and calculated trajectories in the yz plane for $0 \leqslant t \leqslant 4\pi$ for the adaptation process due to the change in m_a were the same as in Fig. 9. Again, there was almost no deviation of the calculated path from the desired path during the adaptation process, or after it was completed. The reason for this may be related to the fact that a large value for $\gamma_1 = 400$ was chosen, which caused a very rapid convergence of $\hat{m}_a$ to m_a.

4.6 Case 5: links with the masses

This case is very similar to the case in Section 4.5 where step changes in m_b were assumed. The difference, however, was the change in the physical parameters introduced earlier into equation (37) which were

$$m_a = 1 \text{ kg}, \qquad 3 \leqslant m_b \leqslant 4 \text{ kg}$$
$$m_1 = 1 \text{ kg}, \qquad m_2 = 1 \text{ kg} \tag{39}$$

In particular, the links of the manipulator were no longer massless, and the mass at the tip of the manipulator was much larger than the mass at the elbow joint unlike the previous cases.

For the case shown in Fig. 16, the estimated parameters were set to

$$\hat{m}_a = 1, \qquad \hat{m}_b = 3.5$$

initially, and the mass at the tip of manipulator changed from $m_b = 4$ to $m_b = 3.0$ alternatively at each half-cycle of the elliptical trajectory with $\gamma_1 = 500$ and $\gamma_2 = 1500$. Again, this figure indicates that the adaptation law resulted in the convergence of the unknown parameter $\hat{m}_b$ to its new value in a fraction of a second. The unknown parameter $\hat{m}_a$ also converged to its true value shortly after the disturbance due to the change in m_b. The desired and calculated trajectories in the yz plane for $0 \leqslant t \leqslant 4\pi$ for the adaptation process due to this change in m_b were the same as in Fig. 9. A more complicated path than the elliptical trajectory was used in reference [**21**].

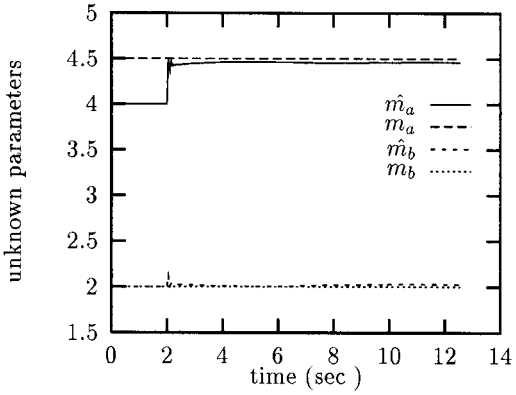

Fig. 15 Adaptation of the estimated parameters with change in m_a with $\gamma_1 = 800$ and $\gamma_2 = 200$ for case 4

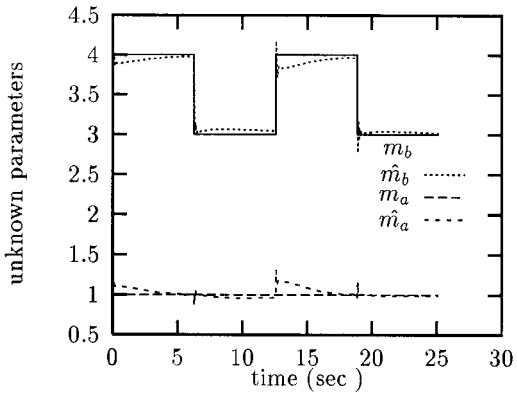

Fig. 16 Adaptation of the estimated parameters with change in m_b with $\gamma_1 = 500$ and $\gamma_2 = 1500$ for case 5

5 CONCLUSIONS

A stable adaptive control approach for a TLRM was presented. Since the dynamics of the manipulator were available, they were used for a non-linear model-based control algorithm. In deriving the dynamic equation of motion, all the physical parameters of the manipulator, including the distributed masses of the links, were considered. Simulation results were presented, which showed the effectiveness of the adaptive control approach for trajectory following and parameter estimation. It is believed that this approach may be used for manipulators with flexible links with the help of the finite element method and some modifications.

ACKNOWLEDGEMENTS

Financial support for this study was provided by a National Science and Engineering Research Council operating grant.

REFERENCES

1 **Ortega, R.** and **Spong, M. W.** Adaptive motion control of rigid robots: a tutorial. *Automatica*, 1989, **25**(6), 877–888.
2 **Middleton, R. H.** and **Goodwin, G. C.** Adaptive computed torque control for rigid link manipulators. *Systems Control Lett.*, 1988, **10**, 9–16.
3 **Fotouhi-C., R., Szyszkowski, W.** and **Nikiforuk, P.** Some aspects of adaptive control of rigid manipulators. In Proceedings of the 18th IASTED International Conference on *Modelling, Identification and Control*, Innsbruck, Austria, 1999, pp. 402–404.
4 **Craig, J. J., Hsu, P.** and **Sastry, S. S.** Adaptive control of mechanical manipulators. *Int. J. Robotics Res.*, 1987, **6**(2), 16–28.
5 **Spong, M. W.** and **Ortega, R.** On adaptive inverse dynamics control of rigid robots. *IEEE Trans. Autom. Control*, 1990, **35**(1), 92–95.
6 **Dawson, D. M.** and **Lewis, F. L.** Comments on 'On adaptive inverse dynamics control of rigid robots'. *IEEE Trans. Autom. Control*, 1991, **36**(10), 1215–1216.
7 **Bayard, D. S.** and **Wen, J. T.** New class of control laws for robotic manipulators. Part 2: adaptive case. *Int. J. Control*, 1988, **47**(5), 1387–1406.
8 **Liu, M.** Computed torque scheme based adaptive tracking for robot manipulators. In Proceedings of the IEEE International Conference on *Robotics and Automation*, Nogaya, Japan, 1995, pp. 587–590 (IEEE, New York).
9 **Sadegh, N.** and **Horowitz, R.** Stability and robustness analysis of a class of adaptive controllers for robotic manipulators. *Int. J. Robotics Res.*, 1990, **9**(3), 74–92.
10 **Slotine, J.-J. E.** and **Li, W.** On the adaptive control of robot manipulators. *Int. J. Robotics Res.*, 1987, **6**(3), 49–59.
11 **Slotine, J.-J. E.** and **Li, W.** Adaptive manipulator control: a case study. *IEEE Trans. Autom. Control*, 1988, **33**(11), 995–1003.
12 **Qu, Z., Dawson, D. M.** and **Dorsey, J. F.** Exponentially stable trajectory following of robotic manipulators under a class of adaptive controls. *Automatica*, 1992, **28**(3), 579–586.
13 **Spong, M. W.** Adaptive control of robot manipulators: design and robustness. In Proceedings of the American Control Conference, San Francisco, California, 1993, pp. 2826–2830.
14 **Slotine, J.-J. E.** and **Li, W.** *Applied Nonlinear Control*, 1991 (Prentice-Hall, London).
15 **Berghuis, H., Ortega, R.** and **Nijmeijer, H.** A robust adaptive robot controller. *IEEE Trans. Robotics Automation*, 1993, **9**(6), 825–830.
16 **Kaneko, K.** and **Horowitz, R.** Repetitive and adaptive control of robot manipulators with velocity estimation. *IEEE Trans. Robotics Automation*, 1997, **13**(2), 204–217.
17 **Burg, T., Dawson, D. M.** and **Vedagarbha, P.** A redesigned dcal controller without velocity measurements: theory and demonstration. *Robotica*, 1997, **15**, 337–346.
18 **Paden, B.** and **Panja, R.** Globally asymptotically stable 'pd+' controller for robot manipulators. *Int. J. Control*, 1988, **47**(6), 1697–1712.
19 **Craig, J. J.** *Adaptive Control of Mechanical Manipulators*, 1988 (Addison-Wesley, Reading, Massachusetts).
20 **Markiewicz, B.** Analysis of the computed torque drive method and comparison with conventional position servo for a computed-controlled manipulator. Technical memorandum 33-601, Jet Propulsion Laboratory, 1973.
21 **Fotouhi-C., R., Nikiforuk, P.** and **Szyszkowski, W.** Combined trajectory planning and parameter identification of a two-link rigid manipulator. In Proceedings of the ASME Design Engineering Technical Conference, Atlanta, Georgia, 1998 (American Society of Mechanical Engineers, New York).

APPENDIX 1

Automatic calculation of the control gain $\boldsymbol{\Gamma}$

Equations (16), (17) and (19) to (21) can also be used to determine a rational relationship between the magnitudes of the gains $\mathbf{K}_v$ and $\mathbf{K}_p$ in the matrix $\mathbf{A}$ and the magnitudes of γ_i in the matrix $\boldsymbol{\Gamma}$. It is suggested that the matrices $\boldsymbol{\Gamma}$ and $\boldsymbol{\Omega}$ are chosen in such a way that in equation (17) the term containing the tracking error $\boldsymbol{x}$ and the term containing the parameter estimation error $\boldsymbol{\Phi}$ are approximately equal:

$$\boldsymbol{\Phi}^{\mathrm{T}}\boldsymbol{\Gamma}^{-1}\boldsymbol{\Phi} \approx \boldsymbol{x}^{\mathrm{T}}\boldsymbol{\Omega}\boldsymbol{x} \tag{40}$$

This is not a simple task since, during the manoeuvre only $\boldsymbol{x}$ can be calculated. However, $\boldsymbol{\Phi}(t)$ is related to $\boldsymbol{x}$ through equation (20):

$$\dot{\boldsymbol{\Phi}}(t) = -\boldsymbol{\Gamma}\mathbf{W}^{\mathrm{T}}\hat{\mathbf{M}}^{-1}\boldsymbol{e}_{\mathrm{f}} = -\boldsymbol{\Gamma}\mathbf{U}\mathbf{C}\boldsymbol{x} = -\boldsymbol{\Gamma}\mathbf{U}\mathbf{B}^{\mathrm{T}}\boldsymbol{\Omega}^{\mathrm{T}}\boldsymbol{x}$$

where $\mathbf{U} = \mathbf{W}^{\mathrm{T}}\hat{\mathbf{M}}^{-1}$. After integration,

$$\boldsymbol{\Phi} = -\int_0^t \boldsymbol{\Gamma}\mathbf{U}\mathbf{B}^{\mathrm{T}}\boldsymbol{\Omega}^{\mathrm{T}}\boldsymbol{x}\,\mathrm{d}t + \boldsymbol{\Phi}_0$$

where $\boldsymbol{\Phi}_0 = \boldsymbol{\Phi}(0)$ is the initial parameter estimation error. If the errors $\boldsymbol{x}$ and $\boldsymbol{\Phi}$ are reduced to zero in time t_x (this time is referred to as the parameter identification period and can be a fraction of the period of the manoeuvre), and the rates at which $\boldsymbol{x}$ and $\mathbf{U}$ change are slow, then $\boldsymbol{\Phi}_0$ is approximately estimated as

$$\boldsymbol{\Phi}_0 = \int_0^{t_x} \boldsymbol{\Gamma}\mathbf{U}\mathbf{B}^{\mathrm{T}}\boldsymbol{\Omega}^{\mathrm{T}}\boldsymbol{x}\,\mathrm{d}t \approx \frac{\boldsymbol{\Gamma}\mathbf{U}_0\mathbf{B}^{\mathrm{T}}\boldsymbol{\Omega}^{\mathrm{T}}\boldsymbol{x}_{\mathrm{m}}t_x}{2}$$

where $\boldsymbol{x}_{\mathrm{m}}$ is the maximum tracking error and $\mathbf{U}_0$ is defined at zero time. The term $e_{\boldsymbol{\Phi}}(0)$ containing the parameter estimation error at the beginning of the process can be obtained now as

$$\boldsymbol{\Phi}_0^{\mathrm{T}}\boldsymbol{\Gamma}^{-1}\boldsymbol{\Phi}_0 = \left(\int_0^{t_x} \boldsymbol{x}^{\mathrm{T}}(\boldsymbol{\Gamma}\mathbf{U}\mathbf{B}^{\mathrm{T}}\boldsymbol{\Omega}^{\mathrm{T}})^{\mathrm{T}}\,\mathrm{d}t\right)\boldsymbol{\Gamma}^{-1}\boldsymbol{\Gamma} \times \left(\int_0^{t_x} \mathbf{U}\mathbf{B}^{\mathrm{T}}\boldsymbol{\Omega}^{\mathrm{T}}\boldsymbol{x}\,\mathrm{d}t\right)$$

or

$$\boldsymbol{\Phi}_0^{\mathrm{T}}\boldsymbol{\Gamma}^{-1}\boldsymbol{\Phi}_0 \approx \frac{\boldsymbol{x}_{\mathrm{m}}^{\mathrm{T}}(\boldsymbol{\Omega}\mathbf{B}\mathbf{U}_0^{\mathrm{T}}\boldsymbol{\Gamma}^{\mathrm{T}}\mathbf{U}_0\mathbf{B}^{\mathrm{T}}\boldsymbol{\Omega}^{\mathrm{T}})\boldsymbol{x}_{\mathrm{m}}t_x^2}{4}$$

Then, using equation (40), it may be concluded that

$$\frac{\boldsymbol{\Omega}\mathbf{B}\mathbf{U}_0^{\mathrm{T}}\boldsymbol{\Gamma}^{\mathrm{T}}\mathbf{U}_0\mathbf{B}^{\mathrm{T}}\boldsymbol{\Omega}^{\mathrm{T}}t_x^2}{4} \approx \boldsymbol{\Omega} \tag{41}$$

where the matrix $\boldsymbol{\Omega}$ is specified by equation (30), in which ψ_j can be considered known if the gains $\mathbf{K}_{\mathrm{p}}$ and $\mathbf{K}_{\mathrm{v}}$ are assumed and equation (29) is used. Equation (41) can be used now to estimate $\boldsymbol{\Gamma}$, the gains of the adaptation law (31) in terms of $\mathbf{K}_{\mathrm{p}}$ and $\mathbf{K}_{\mathrm{v}}$ and the desired parameter identification period t_x.

APPENDIX 2

Detail of equations (2) and (35)

The equations of motion of the manipulator as given in equation (2) are

$$a_{11}\ddot{\varphi}_1 + a_{12}\ddot{\varphi}_2 - a_{13}(2\dot{\varphi}_1 + \dot{\varphi}_2)\dot{\varphi}_2 + a_{14}g = \tau_1(t)$$

$$a_{12}\ddot{\varphi}_1 + a_{22}\ddot{\varphi}_2 + a_{13}\dot{\varphi}_1^2 + a_{24}g = \tau_2(t)$$

where

$$a_{11} = p_1 + p_2 + p_5 + p_3 + p_4 + p_6 + 2p_{11}\cos(\varphi_2)$$

$$a_{12} = p_3 + p_4 + p_6 + p_{11}\cos(\varphi_2)$$

$$a_{13} = p_{11}\sin(\varphi_2)$$

$$a_{22} = p_3 + p_4 + p_6$$

$$a_{14} = (p_7 + p_8)\cos(\varphi_1) + (p_9 + p_{10})\cos(\varphi_1 + \varphi_2)$$

$$a_{24} = (p_9 + p_{10})\cos(\varphi_1 + \varphi_2)$$

$$p_1 = m_1 l_{c1}^2, \quad p_2 = I_1, \quad p_5 = (m_2 + m_{\mathrm{a}} + m_{\mathrm{b}})l_1^2$$

$$p_3 = m_2 l_{c2}^2, \quad p_4 = I_2, \quad p_6 = m_{\mathrm{b}} l_2^2$$

$$p_7 = m_1 l_{c1}, \quad p_8 = (m_2 + m_{\mathrm{a}} + m_{\mathrm{b}})l_1$$

$$p_9 = m_2 l_{c2}, \quad p_{10} = m_{\mathrm{b}} l_2$$

$$p_{11} = (m_2 l_{c2} + m_{\mathrm{b}} l_2)l_1$$

As can be seen, the system dynamics of a TLRM has been arranged in such a way that equation (1) is linear with respect to the selected system parameters p_i, $i = 1, \ldots, 11$. The actual manipulator's parameters can be defined using the following linear mapping:

$$(p_1, p_7) \Rightarrow (m_1, l_{c1}), \quad (p_3, p_9) \Rightarrow (m_2, l_{c2}), \quad p_2 \Rightarrow I_1$$

$$(p_6, p_{10}) \Rightarrow (m_{\mathrm{b}}, l_2), \quad (p_5, p_8) \Rightarrow (m_{\mathrm{a}}, l_1), \quad p_4 \Rightarrow I_2$$

This is an important property of rigid manipulators. The dynamics are linear in terms of a suitably selected set of robot parameters, which is sometimes referred to as the linear-in-parameters property. Using this property it is possible to write the left-hand side of equation (1) as

$$\mathbf{M}(\boldsymbol{\varphi}, \boldsymbol{P})\ddot{\boldsymbol{\varphi}} + \boldsymbol{Q}(\boldsymbol{\varphi}, \dot{\boldsymbol{\varphi}}, \hat{\boldsymbol{P}}) = \mathbf{W}(\boldsymbol{\varphi}, \dot{\boldsymbol{\varphi}}, \ddot{\boldsymbol{\varphi}})\boldsymbol{P} \tag{42}$$

If, however, the linear-in-parameters property does not hold for some particular types of manipulator, such as the non-revolute joint robots or flexible manipulators, the approximated equation (11) may be used to calculate the regressor matrix.

When the unknown parameters are $p_1 = m_{\mathrm{a}}$ and $p_2 = m_{\mathrm{b}}$ (as in the simulation examples) the matrix $\mathbf{W}$ in equation (35) is

$$\mathbf{W}_{2\times 2} = \begin{bmatrix} w_{11} & w_{12} \\ 0 & w_{22} \end{bmatrix}$$

where

$$w_{11} = l_1^2\ddot{\varphi}_1 + [l_1\cos(\varphi_1)]g$$

$$w_{12} = [l_1^2 + l_2^2 + 2l_1 l_2\cos(\varphi_2)]\ddot{\varphi}_1 + [l_2^2 + l_1 l_2\cos(\varphi_2)]\ddot{\varphi}_2 - l_1 l_2\sin(\varphi_2)(2\dot{\varphi}_1 + \dot{\varphi}_2)\dot{\varphi}_2 + [l_1\cos(\varphi_1) + l_2\cos(\varphi_1 + \varphi_2)]g$$

$$w_{22} = [l_2^2 + l_1 l_2\cos(\varphi_2)]\ddot{\varphi}_1 + l_2^2\ddot{\varphi}_2 + l_1 l_2\sin(\varphi_2)\dot{\varphi}_1^2 + [l_2\cos(\varphi_1 + \varphi_2)]g$$